PCCP

Accepted Manuscript

ROYAL SOCIETY OF CHEMISTRY

www.rsc.org/pccp

Nanoscale

RSCPublishing

ARTICLE

Effective AC needleless and collectorless electrospinning for yarn production

Cite this: DOI: 10.1039/x0xx00000x

P. Pokorny,[a] , E. Kostakova,[a] F. Sanetrnik,[a,c] P. Mikes,[a,c] J. Chvojka,[a,c] T. Kalous,[a] M. Bilek,[b,c] K. Pejchar,[b,c] J. Valtera,[b,c] and D. Lukas[a,c]

Received 00th January 2012,
Accepted 00th January 2012

DOI: 10.1039/x0xx00000x

www.rsc.org/

Nanofibrous materials are essential components for a range of applications, particularly in the fields of medicine and material engineering. These include protective materials, sensors, cosmetics, hygiene, filtration and energy storage. The most widely used and researched technology in these fields is electrospinning. This method of producing fibers yields highly promising results thanks to its versatility and simplicity. Electrospinning is employed in multiple forms, among which needle and needleless direct current (DC) variants are the most distinctive. The former is based on the generation of just one single jet from a nozzle; hence this fabrication process is not very productive. The latter uses the destabilization of free liquid surfaces by means of an electric field, which enhances the throughput since it produces numerous jets, emitted from the surfaces of rollers, spheres, strings and spirals. However, although some progress in total producibility has been achieved, the efficiency of the DC method still remains relatively low. A further drawback of DC electrospinning is that both variants need a collector, which makes it difficult to combine DC electrospinning easily with other technologies due to the presence of the high field strength within the entire spinning zone. This paper describes our experiments with AC electrospinning. We show that alternating current (AC) electrospinning based on a needleless spinning-electrode provides a highly productive smoke-like aerogel composed of nanofibers. This aerogel rises rapidly from the electrode like a thin plume of smoke, without any need for a collector. Our work shows that AC needleless electrospinning gains its efficiency and collector-less feature thanks to the creation of a perpetually charge-changing virtual counter-electrode composed of the nanofibers emitted. High-speed camera recordings demonstrate the formation mechanism of the nanofibrous plume, which is wafted by an electric wind. This wind's velocity field is experimentally investigated. One potential use of AC needleless electrospinning is demonstrated here by spinning it into a yarn.

Introduction

One of the methods currently available for the production of fibrous nanostructures, electrospinning, is a unique technology not only because of its operational simplicity, but since it can also be effectively scaled up to industrial level. Electrospinning usually has two variants: needle and needleless. The needle variant, which has a limited production rate in terms of unit grams per hour, prevailed in the eighties and nineties. Recently, more productive needleless electrospinning technologies have been developed based on the creation of numerous self–organized jets emerging from free liquid surfaces [1,2]. Our experiments have shown that further enhancement of this technology can be achieved using a combination of AC high voltage and a needleless spinning-electrode.

Over the past decade, little research has been carried out into AC electrospinning, in contrast to the numerous detailed studies of its DC variant. The few studies available on AC electrospinning have focused on needle electrospinning processes driven by voltages ranging from 5 kV up to 10 kV [3,4,5]. Our AC electrospinning apparatus consists of a 100 mm long metallic rod, 10 mm in diameter, employed as a spinning-electrode. The top of the rod is supplied with a polymeric solution using an infusion syringe pump. For the experiments, a 50 Hz line AC voltage was applied to the rod through a variable transformer with a maximal root mean square output of 30 kV. The apparatus works without an electrically active collector (Figure 1a,b). Poly(vinyl butyral) (PVB) and Polyacrylonitrile (PAN) were chosen as prototypical polymers, since they can be used for electrospinning at moderate potentials.

Experimental

Our AC electrospinning set-up showed fiber formation occurring at a critical voltage of 15.8 ±7 kV and an optimum operating voltage of 30 kV for both PVB and PAN solutions. After switching the field on, the initiation of numerous jets could be seen forming (Figure 1c). The solvent evaporating from the jets produced strands of solid nanofibers. These nanofibers formed a plastic aerogel that bears a strong resemblance to a plume of wispy smoke, which rises up from the spinning-electrode (Figure 1d), (Supplementary Information 1). Inside the plume, the nanofibers become entangled with each other. The nanofibrous plume can therefore be easily taken hold of and gently manipulated with an appropriate tool. Moreover, this rising column of nanofibers is "compact", in the sense that no nanofiber segment is able to escape from it. The column can be wound up into continuous ligaments, piled up on a flat surface or twisted into a yarn. At the same time, it is extremely sticky and cannot move along any surface it makes contact with. A similar aerogel consisting of carbon nanotubes was produced by Windle *et al.*[6] and was called 'elastic smoke'. After much consideration, we decided upon the term "nanofibrous plume", since this expression best conveys the peculiar mechanical properties of the nanofibrous aerogel produced by our AC electrospinning method. This, then, is the term we use throughout the paper.

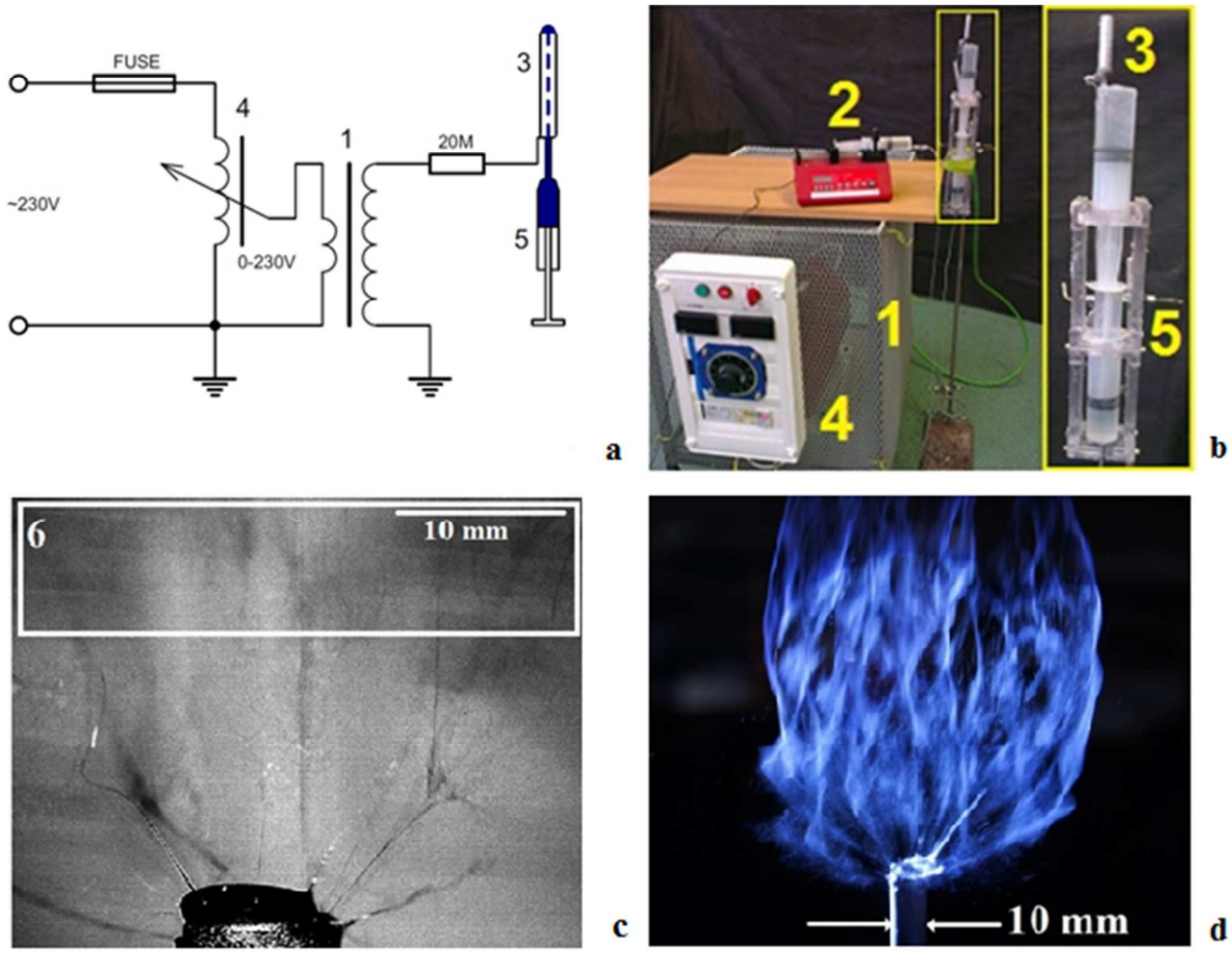

Figure 1 The apparatus for AC electrospinning. a, b, A schematic diagram and photograph of the AC electrospinning set-up, consisting of a metal rod (3) used as the spinning-electrode. The electrode is supplied with a polymeric solution. This is done using a syringe, which is powered by a hydraulic transmission device (5) controlled by an infusion pump (2). The high voltage supply is provided by means of a transformer (1) and a variable transformer (4). The apparatus works without an electrically active collector. **c,** The fibers are formed inside a spinning zone that spans no more than 40 mm from the spinning-electrode. The spinning zone is formed between the top of the spinning-electrode and the virtual counter-electrode (6) composed of the nanofibers, which have been emitted. **d,** The nanofibrous plume composed of PVB nanofibers generated by a rod-shaped spinning-electrode.

The high-speed camera recordings showed that the number of jets per area were of the order of 1 mm^{-2}. This is one order of magnitude higher than conventional electrospinning processes. Maximum throughputs of AC and DC methods for equivalent spinning-electrodes, polymeric solutions and voltage differences are compared in Table 1.

Type of spinning-electrode	AC electrospinning throughput in ml/hour	DC electrospinning throughput in ml/hour
Needle ∅ 0.7 mm	80	1-3
Needleless ∅ 10 mm	180	30

Table 1 Electrospinning throughputs. The maximum throughputs of AC and DC electrospinning variants are compared for PVB and a voltage of 30 kV.

Methods

The AC needleless electrospinning set-up consisted of four components: an ABB KGUG 36 high-voltage transformer with a conversion ratio 36000/230V, a residual-current device, a New Era NE-1000X dosing pump, and a rod electrode. The output voltage was controlled by a Thalheimer-Trafowerke ESS 104 variable transformer, designed for 230V AC input and an output of 0-250V. The maximum output current was 4 A with a capacity (KVA) of 1.2. A hydraulic transmission device (Technical University of Liberec) was used to isolate the pump from the AC high voltage supply.. The transmission was achieved using two syringes, fixed in a polycarbonate holder, facing in opposite directions, with their plungers touching. The first syringe, containing water, was connected by a tube to a linear pump. The second syringe supplied the spinning-electrode with a polymer solution.The two plungers, which touch one another, transmitted the pressure inside the syringes and insulated the water circuit from the polymer solution electrically. Aluminum rod spinning-electrodes with outer diameters of 6, 8 and 10 mm, and of various lengths, spanning from 18 mm up to 150 mm, were used. The polymer solution was fed to the tip of the spinning-electrode via a 3 mm wide coaxial channel. The PVB, Mowital® B 60 H, was obtained from Kuraray America, Inc., and had an average molecular weight of 60,000 amu. A 10 wt% solution was prepared in ethanol-water (9:1 v/v). The polyacrylonitrile PAN was supplied by Sigma-Aldrich and had an average molecular weight of 150,000 amu. A 15 wt% solution of PAN was prepared in dimethylformamide from Penta, Czech Republic. The movement of nanofibers was detected using a high-speed camera system i-SPEED 3 with an F-mount lens connection and a recording frequency of 2000 Hz to obtain a maximum picture resolution of 1280 x 1024 px. The light source used was an ILP-1 with a discharge lamp of 120W at a temperature of 5 600 K and was focused using an optical cable. Analysis of the video obtained was carried out using I-SPEED Suite software. A hot wire anemometer TESTO 425 with a resolution of 0.01 m/s and a range 0 - 20 m/s was used to measure ionic wind velocity. All the experiments were performed at a room temperature of 21±2°C and a humidity rate of 52±5%.

Results and discussion

What follows is a phenomenological description of the fiber formation mechanisms under the AC potential, based on the analysis of high-speed camera videos. The most obvious difference between DC and AC needleless variants of electrospinning is that the latter needs no counter-electrode/collector. Even when a grounded collector was provided, the AC spinning process was not affected by this. Therefore we hypothesize that the AC process possesses some kind of self-organized counter-electrode, which enables the appearance of super-critical field strength values on the polymer solution surface. This strength was estimated to be greater than 2.5 MV/m [1]. We also hypothesize that the self-organized counter-electrode is formed repeatedly in the immediate vicinity of the spinning-electrode. This counter-electrode consists of electrically charged nanofiber segments. The groups of nanofibers created by the spinning-electrode rapidly alternate (every 10 ms) between being either positively or negatively charged. Their electric charge corresponds to the respective positive or negative charge of the currently ongoing voltaic half-wave, generated by the AC power-supply.

The newly-spun nanofibers partially recombine with those that have already formed the virtual counter-electrode. This process is continuously repeated due to the AC nature of the high voltage applied (Figure 1c), (Supplementary Information 2). Alternately-charged nanofibrous groups from successive emissions attract each other to form what is described here as a 'nanofibrous plume' emanating from the virtual collector (Figure 1d). The nanofibrous plume, comprising recombined strands of nanofibers, rose from the rod-shaped spinning-electrode along the direction of its axis. It moved at 0.25 m/s – 0.6 m/s due to an electric wind created by the spinning-electrode [7]. When the nanofibrous plume was at a distance of 2-5 cm from the spinning-electrode, it was internally immobile without any fiber regrouping (Supporting Information 2). Our hypothesis that the virtual collector causes a charge recombination of the nanofibrous groups was supported by our aforementioned observations.

The movement of the nanofibrous plume caused by the electric wind is an important part of the AC collectorless electrospinning technique. The wind does not allow the newly-created nanofibers to be attracted back to the spinning-electrode during the next AC half-wave, when the spinning-electrode polarity is changed. Instead, they are attracted to one another to form groups inside the plume as a result of the Coulomb force, and are then blown away.

Electric, ionic or corona winds are gas flows driven by ions generated by corona discharges and accelerated in an applied electric field [8,9]. Field-accelerated ions transfer momentum to surrounding gas. The electric wind is caused both by DC and AC fields and its velocity depends on actuator geometry, field strength and, in the case of the latter, also on AC frequency. Drews *et al.*[8] observed that during high frequency AC regimes, the electric force causing the wind is localized near the point electrode. Therefore AC coronas can sustain wind velocity independently of electrode separation. Our set-up resembled the so-called "point-plate" actuator[10] with a counter-electrode, i.e., a collector, infinitely distant.

Figure 2a shows the field of vertical components of electric wind velocity created by the spinning-electrode. In this experiment the spinning-electrode had a diameter of 10 mm and a length of 150 mm, and was connected to a 50 Hz AC frequency power supply of the root mean square voltage 30 kV. Velocity values were measured using the hot wire anemometer at an array of points, spanning 400 x 450 mm. This array was situated 250 mm above the spinning-electrode and lay in a plane containing the spinning-electrode axis. The top velocity at the point nearest to the spinning-electrode was 0.57 ± 0.14 m/s. A minimum distance of 250 mm of the measurement area from the spinning-electrode ensured that the hot wire anemometer was protected from a possible electric discharge. The velocities of the electric wind measured at the same point array, without the electric field switched on, were negligible. Their values were 0.01 ±0.01 m/s.

The effect of the electric wind combined with a movement of the nanofibrous plume was also investigated. This was done by tracking polymeric droplets inside the nanofibrous plume as shown in Figure 2b. The software I-SPEED provides us with velocity magnitude values that are plotted in the same figure. Velocity magnitude values

have a significant change of their derivative at a distance of 29 ⌖ 8 mm above the tip of the spinning-electrode, as was measured using 10 tracking trials. Therefore, we assume that the virtual collector was formed at this distance and electric charges of nanofibrous groups were recombined here. The velocity magnitude before the virtual collector steeply decays, while behind it, it is nearly constant, 0.46 ⌖ 0.08 m/s. This value coincides with electric wind velocities measured using the anemometer.

The initiation of AC electrospinning is similar to DC electrospinning regarding the duration and formation of Taylor cones. High speed imaging revealed that the DC as well as the first AC initiations took about 0.0358 s - 0.2486 s, depending on the polymeric solution composition and the voltage applied. However, our research revealed two differences. Firstly, the time for successive and repeated jet creation during AC electrospinning was extremely short. The jets disappeared at the end of each voltaic half-wave and were newly created when the voltage increased. Recordings from the high-speed camera showed that it took only 0.0006 s for the jets to form again (Supplementary information 3). In addition, the large conical protuberances (Taylor cones) did not appear in the case of AC electrospinning. Instead, the jets emanated directly from a seemingly relaxed polymeric droplet attached to the spinning-electrode (Figure. 3a).

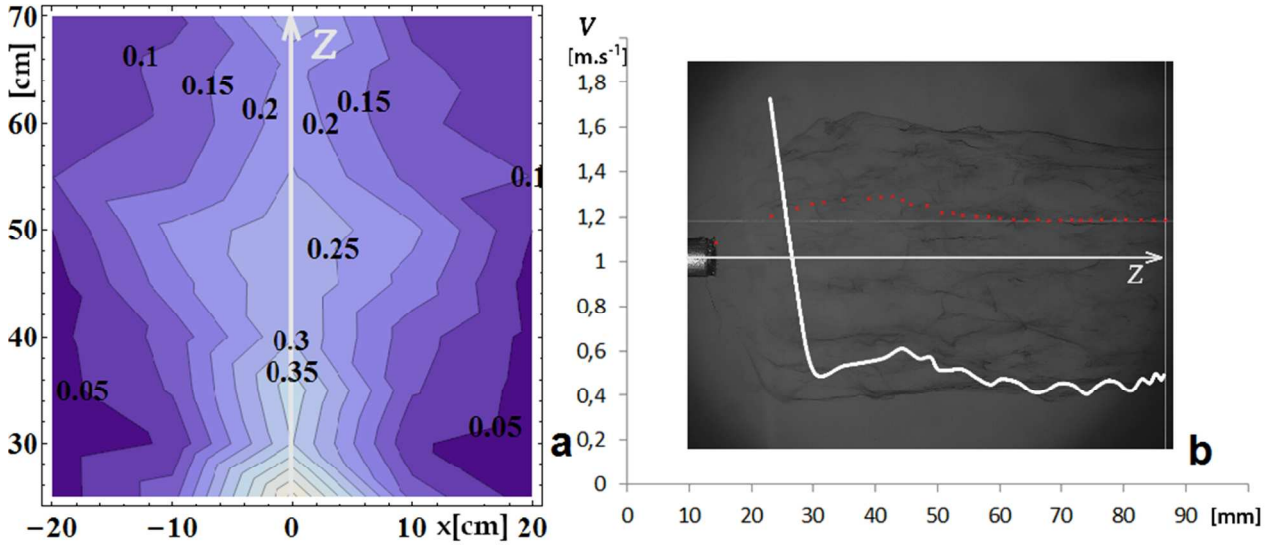

Figure 2 Electric wind measurements. a, Contour plot of vertical components of the electric wind velocity in m/s created by the spinning-electrode with a diameter of 10 mm whose axis coincidences with the *z* coordinate. This is connected to a 50 Hz AC frequency power supply of a root mean square voltage of 30 kV. The tip of the spinning-electrode is positioned at $z = 0$. **b,** The typical track of a polymeric droplet inside the nanofibrous plume, recorded using a high-speed camera. Included is a plot of the velocity magnitude values *v* as a function of the z-axis distance from the spinning-electrode, which exhibits an abrupt change of the velocity derivative close to the distance z = 30 mm.

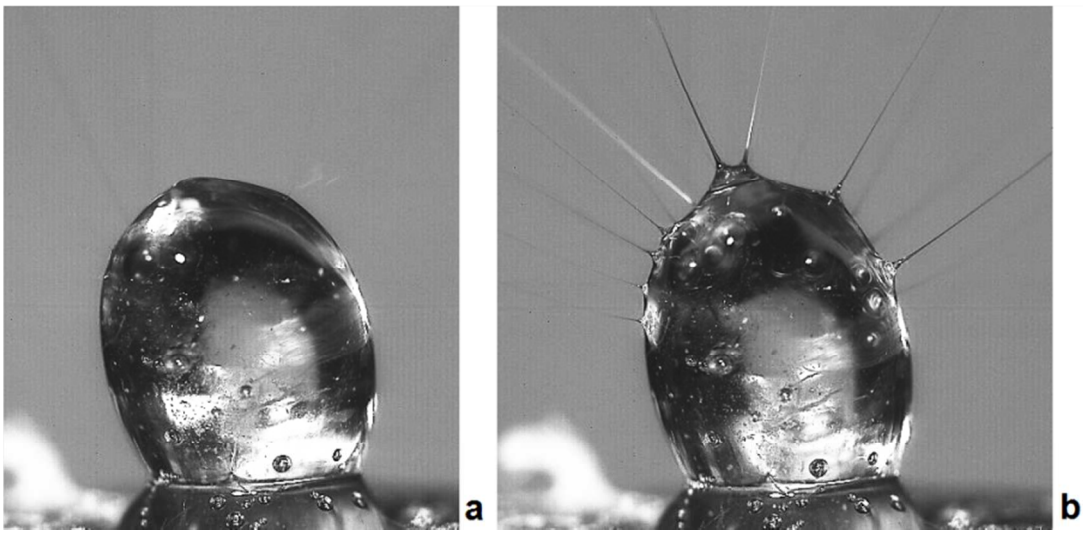

Figure 3 Jet formation in AC Electrospinning. In repeated AC initiation, the time delay from the moment when (a) the jets have dispersed until b) the new jets have formed is only 0.0006 s.

Nanoscale RSCPublishing

ARTICLE

Figure 4a shows the microscope image of a PVB nanofibrous material produced under AC conditions with a potential of 20 kV. Fibers in this material are highly tortuous (inter-twined) due to the mechanism of their creation, in which positively and negatively charged jet segments are mutually attracted. AC electrospun PAN material exhibits similar morphological features (Figure 4d). The most striking feature of AC nanofibers is their varicose appearance. Varicosity is expressed here as a plot of fiber diameter measured along a fiber length. The varicosity of AC and DC electrospun PVB nanofibers are compared, in order to show the differences (Figure 4c). These AC and DC nanofibrous samples were prepared from the same PVB solution and a similar voltage was applied in their production.

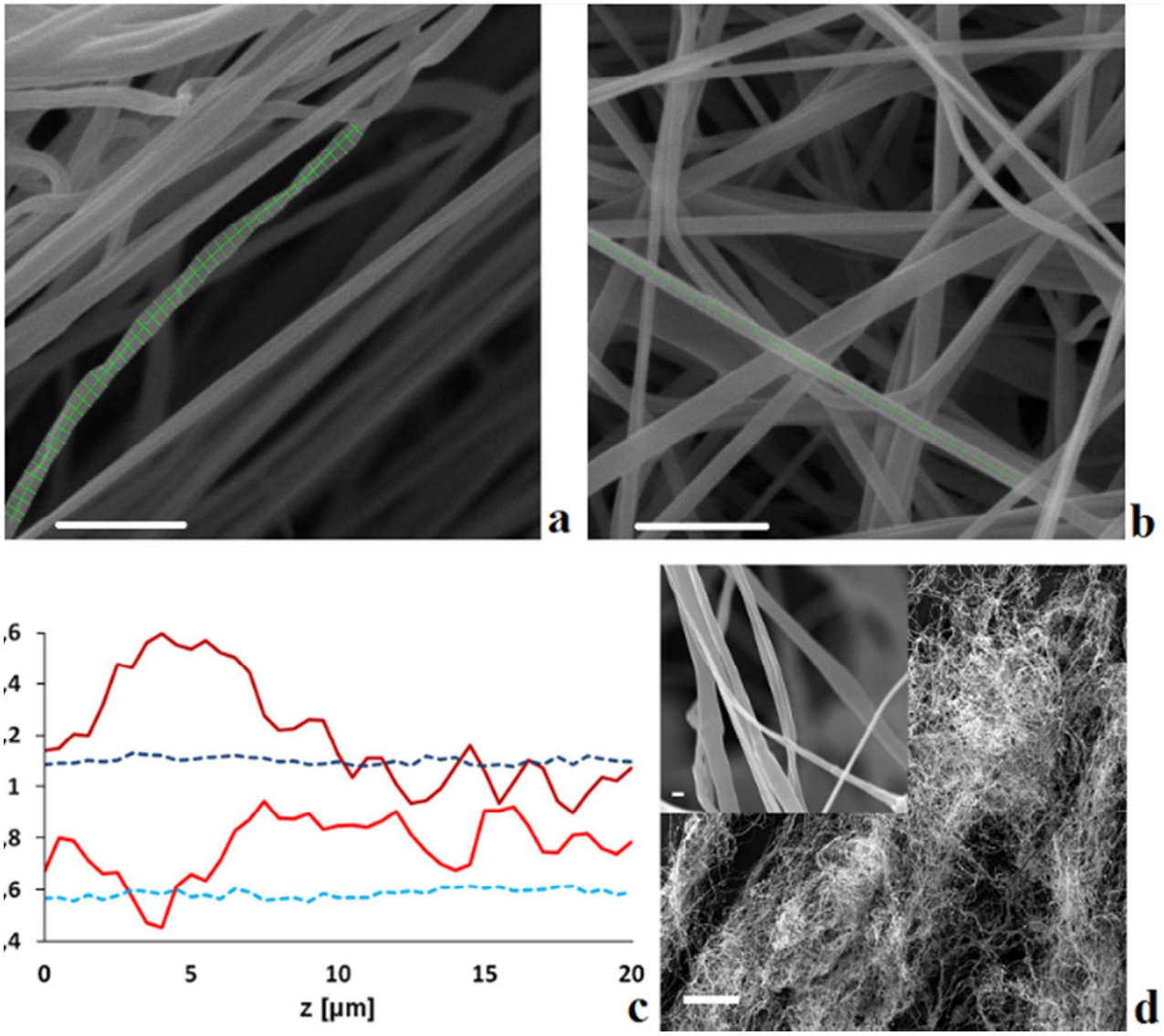

Figure 4 SEM images of AC electrospun materials. a, A SEM image of PVB nanofibrous material produced by AC needleless electrospinning (scale bar 5 µm). **b,** PVB fibers electrospun, using a DC method with the same rod-shaped spinning-electrode, from the same solution and at the same voltage as the former AC material (scale bar 5 µm). **c**, Varicosity of two randomly-selected AC (continuous curves) and two DC (dashed curves) fibers evaluated as diameter measurements along fiber axes. **d**, A SEM image of AC electrospun PVB fibers as an example of nanofibrous material produced from organic solvents using the technology described. (scale bar 500 µm and 1 µm for the inset image).

Nanoscale RSCPublishing

ARTICLE

Our investigations into AC electrospinning have revealed that the nanofibrous plume has mechanical properties which make it eminently suitable for twisting to form a yarn. This plume is enormously ductile and hence its ends can be attached to a circular brush which, in turn, is attached to an FBS 115/E Proxxon Rotary Tool. This tool is capable of a rotation speed of between 5,000 and 20,000 rpm. The number of twists per unit length allows the formation of nanofibrous yarns of a predetermined density (Supplementary Information 4). Similar short-yarn spinning technology has been developed for short electrospun nanofibrous yarns gathered from a special multi-plate rotating collector [11]. SEM images of PVB yarns electrospun from the nanofibrous plume are introduced in Figure 4a-c. In addition, the average fiber diameter of the AC-spun PVB nanofibers spun onto the yarn is far less than 1 μm.

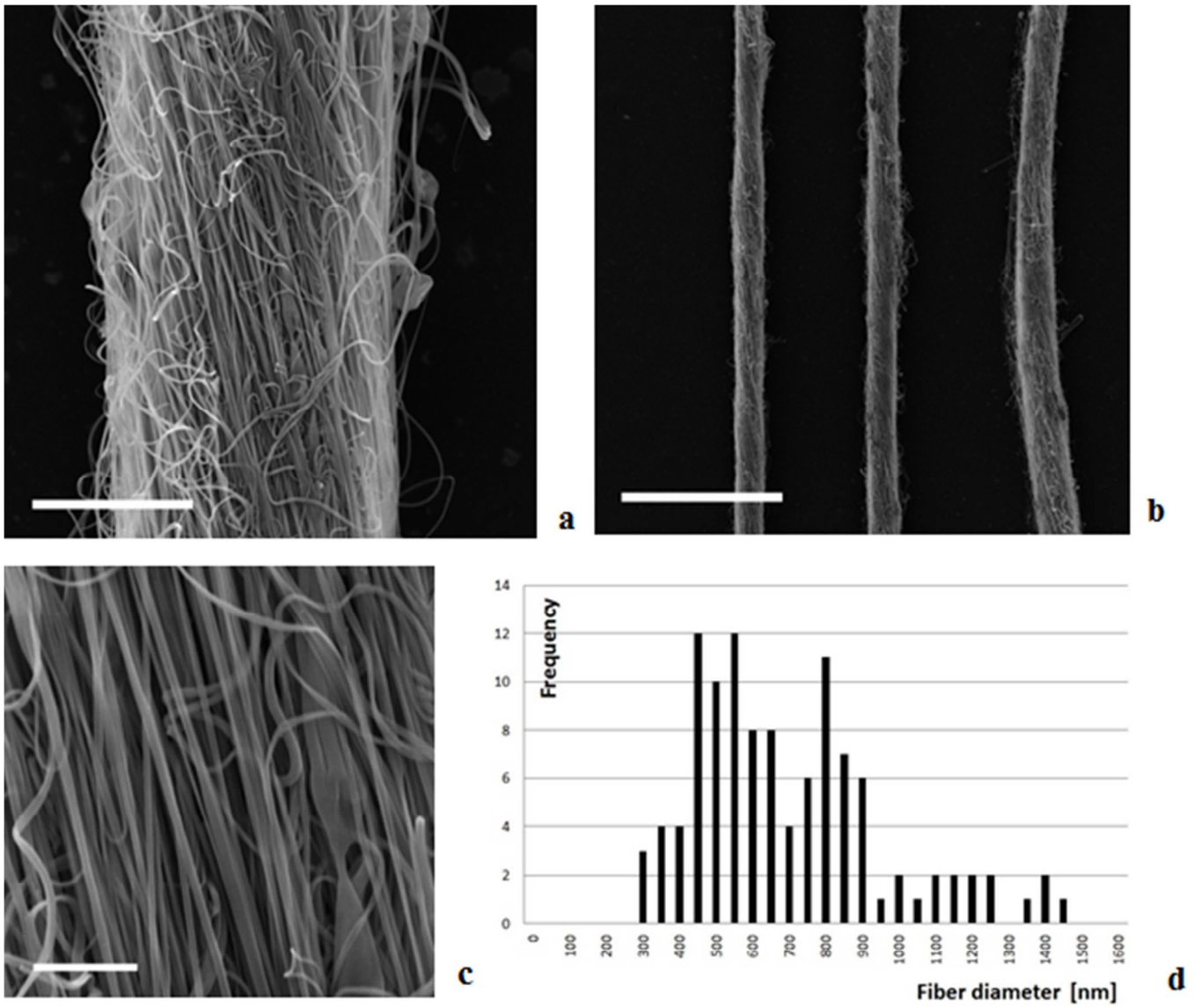

Figure 5 SEM images of PVB yarns spun from the nanifibrous plume and a fiber diameter histogram. a, Nanofibers yarn was directly produced from the nanofibrous plume and formed using the circular brush attached to the Proxxon Rotary Tool (scale bar 50 μm). **b,** Three yarn pieces taken from the ends and the middle part of a 5 m long yarn, which show good reproducibility of its diameter (scale bar 500 μm). **c,** The detailed picture of the same material (scale bar 10 μm). **d**, Histogram of fiber diameter in the PVB needleless AC electrospun yarn.

Nanoscale RSCPublishing

ARTICLE

Conclusions

In summary, our experiments have shown that AC electrospinning combined with an appropriately-shaped, needleless spinning-electrode is highly efficient at generating a dense plume of nanofibers. The efficiency of this method is achieved by means of the virtual counter-electrode. This virtual counter-electrode formed by a cloud of nanofibers is recreated periodically in each half-wave of the AC cycle. The recombined pieces of newly-formed nanofibers are then moved by the electric wind to create the nanofibrous plume. The AC needleless electrospinning method introduced in this work has the potential to be linked to existing technologies. There are two significant reasons for this. Firstly, there is no obstacle, such as a collector, along the spinning line. AC electrospinning can therefore be used for the mass production of nanofibers thanks to its remarkable throughput. In addition, the immediate product of AC electrospinning is a compact aerogel (i.e. the plume of nanofibers), which can be readily manipulated for further processing. As an example of this, we have introduced a promising application of the nanofibrous plume, namely the production of nanofibrous yarns.

With the rapid developments in nano-science and nanotechnology, yarns composed of nanofibers may open up a whole range of new possibilities. One such application is the production of a porous artificial proboscis, which could be used to collect tiny liquid samples[11]. Nanofibrous yarns are also the basic material element for the development of nanofibrous structures, such as woven and knitted fabrics, macrame and laces[12], whose mechanical, sorption and filtration properties will significantly differ from that of conventional textiles. Nanofibrous textiles may also have great potential uses in the field of medicine. They are able to meet the criteria for medical applications[13] largely as a result of the unique characteristics mentioned here in this paper.

Acknowledgements

We thank Lubomir Kocis, EGU HV Laboratory a.s., for his assistance in the initial experiments and for the fruitful discussions we had with him. The authors acknowledge the support of GACR, Grant no. P208/12/0105.

Notes and references

[a] Faculty of Textile Engineering, Technical University of Liberec, Studentska 2, Liberec 1, Czech Republic, 461 17.

[b] Faculty of Mechanical Engineering, Technical University of Liberec, Studentska 2, Liberec 1, Czech Republic, 461 17.

[c] Centre for Nanomaterials, Advanced Technologies and Innovation of Technical university of Liberec, Studentska 2, Liberec 1, Czech Republic, 461 17.

Electronic Supplementary Information (ESI) available: [Supplementary Information 1: A 'nanofibrous plume' emanating from the virtual collector, Supplementary Information 2: The nanofibrous plume, comprising recombined strands of nanofibers, moves away from the rod spinning-electrode, Supplemetary Information 3: Successive and repeated jet creations during AC electrospinning, Supplementary Information 4: A promising application for nanofibrous plume is in the production of nanofibrous yarns]. See DOI: ??????????????

1 D. Lukas, A. Sarkar, *Journal of Applied Physics*, 2008, **103**, 0843091, DOI: 10.1063/1.2907967.

2 T. Miloh, B. Spivak and A.L. Yarin, *Journal of Applied Physics,* 2009, **106**, 114910, DOI: 10.1063/1.3264884.

3 R. Kessick, J. Fenn and G. Tepper, *Polymer*, 2004, **45**, 2981, DOI: 10.1016/j.polymer.2004.02.056.

4 S. Sarkar, S. Deevi and G. Tepper, *Macromolecular rapid communications*, 2007, **28**, 1034, DOI: 10.1002/marc.200700053.

5 S. Maheshwari, H.C. Chang, *Advanced Materials*, 2009, **21**, 349, DOI: 10.1002/adma.200800722.

6 Y.-L Li, I.A. Kinloch and A. Windle, *Science,* 2004, **304**, 276, DOI: 10.1126/science.1094982.

7 A.M. Drews, L. Cademartiri, G.M. Whitesides and K. J. M. Bishop, *Journal of Applied Physics*, 2014, **114**, 143302, DOI: 0.1063/1.4824748.

8 A.M. Drews L. Cademartiri, G.M. Whitesides, K.J.M. Bishop, *Journal of Applied Physics*, 2013, **114**, 143302, DOI: 10.1063/1.4824748.

9 B.A. Kozlov, V. I. Solovyov, *Technical Physics,* 2007, **52**, 892–897, DOI:10.1134/S1063784207070109.

10 L.B. Loeb, *Electrical Coronas*, University of California Press, Berkeley, 1965.

11 Ch.-Ch. Tsai, P. Mikes, T. Andrukh, E. White, D. Monaenkova, O. Burtovyy, R. Burtovyy, B. Rubin, D. Lukas, I. Luzinov, J.R. Owens and K..G. Kornev, *Nanoscale*, 2011, **3**, DOI: 10.1039/c1nr10773a.

12 U. Ali, Y. Zhou, T. Lin, *Nanofibers – Production, Properties and Functional Applications*, *Electrospinning of continuous nanofiber bundles and twisted nanofiber yarn*, 2011, DOI: 10.5772/25059.

13 V. Bartels, *Handbook of medical textiles, Woodhead Publishing Series in Textiles*, Elsevier, 2011, ISBN 085709369X.